



CrossMark  
click for updates

Cite this: DOI: 10.1039/c4cy00969j

Received 25th July 2014,  
Accepted 2nd September 2014

DOI: 10.1039/c4cy00969j

www.rsc.org/catalysis

## Bottom-up approach to engineer two covalent porphyrinic frameworks as effective catalysts for selective oxidation†

Weijie Zhang,<sup>a</sup> Pingping Jiang,<sup>\*a</sup> Ying Wang,<sup>a</sup> Jian Zhang<sup>b</sup> and Pingbo Zhang<sup>a</sup>

Two kinds of novel functional covalent organic frameworks were assembled with the porphyrin building block and terephthalaldehyde or squaric acid *via* bottom-up approach. Here, our reported covalent porphyrinic frameworks with coordinated manganese(III) ions (Mn-CPF-1 and Mn-CPF-2) present promising catalytic properties for the selective oxidation of olefins.

Activation of unsaturated bonds is a field of increasing interest in relation to the design of highly active catalysts for selective oxidation reactions. Among them, synthetic metalloporphyrin has long been known as an effective catalyst for oxidation reactions due to its excellent catalytic performance and high product selectivity.<sup>1</sup> However, the application of metalloporphyrin as a catalyst in solution is particularly difficult to achieve because of the formation of catalytically inactive dimers and fast degradation in homogeneous catalysis.<sup>2</sup> Therefore, it is of great significance to circumvent these challenges.

Covalent organic frameworks (COF) are a novel class of porous crystalline organic materials assembled from molecular building blocks by linking light elements (*e.g.* B, C, N, and O) *via* covalent bond formation (boronic acid trimerization, boronate ester formation, the Schiff base reaction, hydrazone and squaraine linkage) in a periodic manner.<sup>3</sup> In terms of catalytic application, COFs have been successfully projected to bridge the gap between heterogeneous materials and homogeneous catalysis.<sup>4</sup> Currently, porphyrins and metalloporphyrins afford ideal synthons for building blocks in the construction of covalent porphyrinic networks analogous to robust inorganic zeolites for versatile application.<sup>5</sup>

To be more precise, the covalent porphyrinic frameworks (CPFs) with accessibility of the open channels can be considered as self-supported catalysts with enhanced performance due to their high-density active sites in the frameworks. The tetrapyrrolic macrocycles of porphyrins play an important role in the design of extended supramolecular lattices because of their robust structure, remarkable thermal and oxidative stability, and unique catalytic properties. In addition, the heterogeneous nature of CPFs can be very useful to separate the catalyst from the products of interest, recover it after simple filtration procedures and finally regenerate it for successive catalytic runs. Therefore, it may be a valuable trial to target efficient heterogeneous catalysts with open coordination frameworks *via* bottom-up strategy, which is essential to catalysis application. Here, the bottom-up method enables direct visualization of the structure and makes it possible to get a detailed insight into the relationship between the structure and the catalytic activity by structural interrogation.

With this background in mind, we reported the development of new CPFs based on the hydrazone and squaraine linkage (Fig. 1). It has been previously studied that condensation of hydrazide with aldehyde<sup>6</sup> or squaraine<sup>7</sup> was a thermodynamically controlled reaction. During this reaction, the formation of hydrazone or squaraine derivatives and water by-products proceeded. Accordingly, we employed *meso*-tetra(4-hydrazidocarbonylphenyl)porphyrin (Fig. 1, THCPP) with four hydrazide groups at the periphery as the aldehyde or squaraine component to condense with hydrazine, with the aim of demonstrating the feasibility of the strategy and features of a new class of CPFs. Furthermore, the crystal data of THCPP (Fig. S1†) obtained by a solvent diffusion method substantiated the point that the macrocycles of porphyrin units could be classified as 2D-C<sub>4</sub> blocks<sup>3c</sup> on a simplified symmetry notation with a rigid nature and discrete bonding direction of arenes in order to make aromatic  $\pi$  systems.

All CPFs were synthesized by solvothermal reactions (see the ESI†). In order to introduce catalytically active sites

<sup>a</sup> The Key Laboratory of Food Colloids and Biotechnology, School of Chemical and Material Engineering, Jiangnan University, Wuxi 214122, PR China.

E-mail: ppjiang@jiangnan.edu.cn

<sup>b</sup> School of Chemistry and Environmental Science, Lanzhou City University, Lanzhou 730000, PR China

† Electronic supplementary information (ESI) available: HNMR, FT-IR, PXRD, TG analysis, crystal data and catalytic details. CCDC 955396. See DOI: 10.1039/c4cy00969j

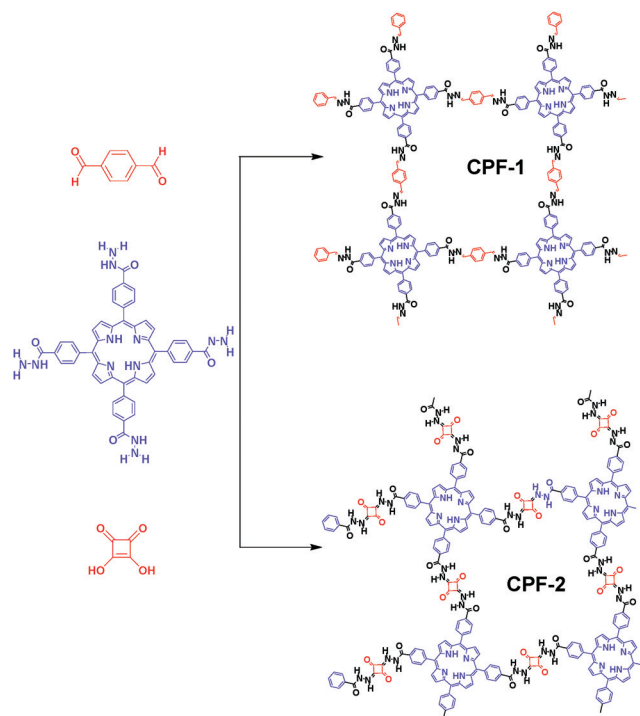


Fig. 1 Schematic representation of molecular building blocks of CPF-1 and CPF-2.

into monomers, metal–porphyrin complexation was employed. As expected, the resultant Mn–HTCPP showed characteristic peaks as  $m/z = 899$  in the MALDI-MS spectra (Fig. S3†). CPF-1 and CPF-2 were obtained as purple solids in 60% and 55% isolated yields, respectively. Mn–CPF-1 and Mn–CPF-2 were obtained as green powder in 52% and 46% yields, respectively. As shown in Fig. S4 and S5,† the FT-IR spectra of CPF-1 and Mn–CPF-1 showed stretching modes at  $1660\text{ cm}^{-1}$  that are characteristic of C=N moieties. For CPF-2 and Mn–CPF-2, the FT-IR exhibited a vibration band at  $1521\text{ cm}^{-1}$ , which is characteristic of a C=O band from squaraine (SQ).

The crystalline structure of the synthesized CPF materials was resolved by XRD measurements in conjunction with structural simulation. Atomic positions and cell sizes of modelled COF layers were optimized using Material studio software. XRD studies on CPF-1 and CPF-2 in Fig. S6 and S7† indicated certain accordance between experimental patterns and the simulated patterns based on the modelled structure. Although the intensities of the XRD patterns for CPF-1 and CPF-2 were poor, the experimental XRD patterns of CPF-1 and CPF-2 also partly matched well with the simulated pattern of the AB stacking model in Fig. S6 and S7† relative to the AA stacking model. Obviously, it was still not yet clear for other diffraction peaks ( $40^\circ > 2\theta > 15^\circ$ ) in CPFs. The cross-linking of CPFs may give rise to uncertain conformation. Nevertheless, Mn–CPF-1 and Mn–CPF-2 did not reveal any obvious diffraction peaks under the same solvothermal growth conditions, implying that they were composed of an amorphous network. This was probably due to the different solution between porphyrins and metalloporphyrins.

Compounds CPF-1 and CPF-2 both exhibited a typical type III isotherm with surface areas of  $158\text{ m}^2\text{ g}^{-1}$  for CPF-1 and  $92\text{ m}^2\text{ g}^{-1}$  for CPF-2 (Fig. S8†). The prepared COFs showed  $\text{N}_2$  adsorption isotherms with low surface areas. It can be speculated that these COFs adopt a thin-layer morphology. Due to the thin-layered structures, long-range pore formation is hindered, rendering  $\text{N}_2$  adsorption possible only in the shallowest, most accessible pores.<sup>8</sup> Alternatively, it may be helpful to prepare the crystalline CPF-1 or CPF-2 first, subsequently introducing Mn to get a Mn catalyst with a crystalline structure. These studies will be reported separately in the near future.

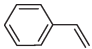
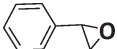
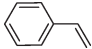
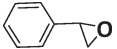
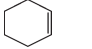
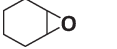
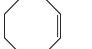
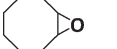
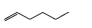
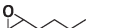

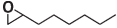


FE-SEM revealed that CPF-1 and CPF-2 were composed of a uniform micrometre-scale bet morphology with a dimension of *ca.* 200 nm and a larger particle of *ca.* 0.5–1  $\mu\text{m}$ , respectively (Fig. S9†). Both samples were stable in various solvents. TGA of the activated CPF-1 and Mn–CPF-1 had no obvious weight loss until  $350^\circ\text{C}$  (Fig. S10†). One may notice that the frameworks of CPF-2 and Mn–CPF-2 started to decompose around  $230^\circ\text{C}$ , which can be attributed to a weak thermal stability of squaraine linkage (Fig. S11†).

The inductively coupled plasma atomic mass spectrometry analysis (ICP-MS) results showed that the density of active Mn sites reached as high as  $1.7\text{ mmol g}^{-1}$  for Mn–CPF-1 and  $1.6\text{ mmol g}^{-1}$  for Mn–CPF-2. The Mn content of Mn–CPF was found to be more than 10 times higher than the record reported amount of Mn complex grafted on insoluble materials, like a mesoporous sieve.<sup>9</sup> In this regard, the bottom-up strategy could facilitate a metalloporphyrinic catalyst with a high-density active site, owing to their accessibility, facile derivatization and ability to bind a wide variety of metal ions, like Cu and Fe ions.

Recent research also showed that framework catalysts with an AB-stacked 3D net, constructed by Mn–porphyrin as a bridging linker and Zn as a node, provided accessibility for the Mn(III) active site to a molecular substrate and accordingly exhibited excellent catalytic properties.<sup>10</sup> Thus, we were encouraged to demonstrate the catalytic efficiency of metallic CPF materials. First of all, styrene was employed to investigate their different catalytic performance. Although the conversion of styrene was very high, a selectivity of 68% for Mn–CPF-1 and a selectivity of 60% for Mn–CPF-2 were revealed after 24 h (Table 1, entries 1 and 2). Mn–CPF-1 led to a faster reaction rate compared to Mn–CPF-2 as shown in Fig. S12.† The comparably low selectivity of styrene epoxides was related to the low electron density of styrene which usually reduced their nucleophilicity toward the electrophilic oxygen of porphyrin–Mn(V)=O.

Excellent heterogeneous catalysts should not only have high catalytic activity and selectivity but also be structurally stable and thus be easily recovered for continuous usage. Compound Mn–CPF-1 can be simply recycled by filtration, which was subsequently reused in successive runs (Fig. S13†). Although the reaction rate decreased, the recycled Mn–CPF-1 still exhibited a very high conversion of 96% and a selectivity of 62% when styrene was being used as a substrate, thus

**Table 1** Scope of Mn-CPF-catalysed epoxidation of alkenes<sup>a</sup>

Entry	Substrate	Product	Catalyst	Conversion <sup>b</sup> (%)	Selectivity <sup>c</sup> (%)
1			Mn-CPF-1	99/96 <sup>d</sup>	68/62 <sup>e</sup>
2			Mn-CPF-2	93	60
3			Mn-CPF-1	99	>99
4			Mn-CPF-1	95	>99
5			Mn-CPF-1	81	>99
6			Mn-CPF-1	66	>99
7			Mn-CPF-1	20	>99

<sup>a</sup> Olefin (1.0 mmol), TBHP (1.5 mmol), the catalyst (0.01 mmol), acetonitrile (3.0 mL) and bromobenzene (50 mg) as internal standards sealed in Teflon-lined screw cap vials were stirred at 80 °C for 24 h. <sup>b</sup> Conversion (%). <sup>c</sup> Selectivity (%) was determined by GC using an SE-54 column (50 °C for 1 min, then 10 °C min<sup>-1</sup> up to 140 °C and 140 °C for 15 min). <sup>d</sup> After the third cycle. <sup>e</sup> The by-products were benzaldehyde and benzenacetaldehyde.

indicating that Mn-CPF-1 was indeed a heterogeneous catalyst for styrene epoxidation (Table 1, entry 1).

The catalytic activity of the epoxidation of cyclohexene and cyclooctene with different steric sizes was further investigated under the same conditions (Table 1, entries 3 and 4). Obviously, Mn-CPF-1 exhibited high catalytic activity and selectivity for epoxidation of cyclohexene. However, cyclooctene with a larger steric size led to a reduced conversion, which suggested that the active catalytic sites should be the Mn-porphyrin moieties within the pores of Mn-CPF-1. In order to further understand the steric effect on catalytic efficiency, a range of natural alkenes were selected to be oxidized in this catalytic system. Increasing the length of linear alkenes triggered lower epoxide yield due to the different steric sizes of the substrates (Table 1, entries 5–7).

To confirm the aforementioned claim, we compared the catalytic activities of Mn-CPF-1 with their molecular components of MnCl<sub>2</sub> and Mn-HTCPP under identical reaction conditions. Mn-HTCPP showed quite moderate catalytic activity that could transform 79% of the cyclohexene into cyclohexene oxide (Table 2, entry 2), but it was still not as efficient as heterogeneous Mn-CPF-1 (99% conversion). MnCl<sub>2</sub> showed lower catalytic activity with a conversion of

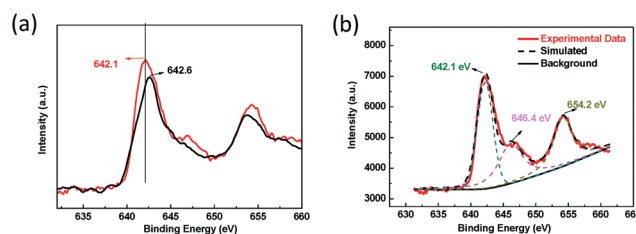
35% (Table 2, entry 3). No increase of trace product was detected after the filtrate from a mixture of Mn-CPF-1 in acetonitrile (Table 2, entry 4). Low epoxide yield was also obtained when no catalytic active sites were added (Table 2, entries 5 and 6). The different catalytic stabilities of Mn-CPF-1 and Mn-HTCPP in the catalytic epoxidation of olefins can be attributed to the homogeneous metalloporphyrin catalyst having very high suicidal inactivation by formation of the catalytically inactive u-oxometalloporphyrin dimers,<sup>11</sup> whereas integration of metalloporphyrins within the pore surfaces of Mn-CPF-1 can significantly enhance and sustain the catalytic activities by blocking formation of the inactive species.

Although Mn-CPF-1 showed superior catalytic efficiency compared to Mn-CPF-2, the nature of Mn sites in Mn-CPFs has not been revealed. To identify this point, XPS analysis can help to reveal the oxidant state of Mn sites of molecules in Mn-CPFs. As shown in Fig. 2, one may notice that the peak value of Mn2p<sub>3/2</sub> in Mn-CPF-1 shifted to a higher value of 642.6 eV, with respect to the value of 642.1 eV in Mn-CPF-1 and 642.2 eV in the previous research.<sup>12</sup> In this case, the redox properties of the Mn complexes in Mn-CPF-1 were greatly influenced after being assembled into extended  $\pi$  systems; that is, the charge was positively transferred from the Mn(III) centre to the linkage. There was a desirable

**Table 2** Scope of catalysed epoxidation of cyclohexene<sup>a</sup>

Entry	Catalyst	Conversion <sup>b</sup> (%)	Selectivity <sup>c</sup> (%)
1	Mn-CPF-1	99	>99
2	Mn-HTCPP	79	53
3	MnCl <sub>2</sub>	35	78
4	Filtrate <sup>d</sup>	20	4
5	Blank	19	5
6	CPF	32	7

<sup>a</sup> Olefin (1.0 mmol), TBHP (1.5 mmol), the catalyst (0.01 mmol), acetonitrile (3.0 mL) and bromobenzene (50 mg) as internal standards sealed in Teflon-lined screw cap vials were stirred at 80 °C for 24 h. <sup>b</sup> Conversion (%). <sup>c</sup> Selectivity (%) was determined by GC using an SE-54 column. <sup>d</sup> After catalytic assay for Mn-CPF-1.



**Fig. 2** (a) XPS spectra for the clean Mn-CPF-1 surface, the fresh catalyst (black line) and Mn-CPF-2 (red line) and (b) XPS spectra for Mn-CPF-2, Mn 2p<sub>3/2</sub> and the high-valent oxo region.

catalysis-promoted electronic environment around the Mn(III) center in Mn-CPF-1. Therefore, Mn-CPF-1 possesses a more efficient performance than Mn-CPF-2, which derives from their catalytic data. In Mn-CPF-2, for example, there was a satellite peak at 646.4 and 654.2 eV, respectively, beside the main peak of Mn2p<sub>3/2</sub>. The resulting satellite peak may be attributed to the manganese-oxo species from the surface of the catalyst.

In summary, we successfully constructed two kinds of covalent porphyrinic frameworks based on the crystal structure of HTCPP *via* bottom-up approach, namely, CPF-1 with a hydrazone linkage and CPF-2 linked by the squaraine linkage. After incorporating the catalytic Mn(III) centre into monomers, the catalytic activity was carefully examined. The results showed that Mn-CPF-1 was the most effective among those tested involving homogeneous and heterogeneous systems. Of further importance, a detailed XPS study evidenced that Mn-CPF-1 had a more desirable electronic environment than Mn-CPF-2. This could help to further understand the relationship between the material structure and catalytic activity.

## Acknowledgements

The authors give special thanks to Dr. Liu from East China University of Science and Technology for his help in the analysis of XPS data. This work was supported financially by the National "Twelfth Five-Year" Plan for Science & Technology (2012BAD32B03), the National Natural Science Foundation of China (20903048) and the Innovation Foundation in Jiangsu Province of China (BY2013015-10).

## Notes and references

- (a) P. R. Ortiz de Montellano, *Chem. Rev.*, 2010, **110**, 932; (b) M. Costas, *Coord. Chem. Rev.*, 2011, **255**, 2912.
- T. C. Bruice, *Acc. Chem. Res.*, 1991, **24**, 243.
- (a) A. P. Cote, A. I. Benin, N. W. Ockwig, M. O'Keeffe, A. J. Matzger and O. M. Yaghi, *Science*, 2005, **310**, 1166; (b) S. Y. Ding and W. Wang, *Chem. Soc. Rev.*, 2013, **42**, 548; (c) X. Feng, X. Ding and D. Jiang, *Chem. Soc. Rev.*, 2012, **41**, 6010.
- (a) L. Li, Z. Chen, H. Zhong and R. Wang, *Chem. – Eur. J.*, 2014, **20**, 3050; (b) X. Chen, N. Huang, J. Gao, H. Xu, F. Xu and D. Jiang, *Chem. Commun.*, 2014, **50**, 6161; (c) X. Feng, L. Chen, Y. Dong and D. Jiang, *Chem. Commun.*, 2011, **47**, 1979.
- (a) Z. Xiang, Y. Xue, D. Cao, L. Huang, J. F. Chen and L. Dai, *Angew. Chem., Int. Ed.*, 2014, **53**, 2433; (b) X.-S. Wang, M. Chrzanowski, D. Yuan, B. S. Sweeting and S. Ma, *Chem. Mater.*, 2014, **26**, 1639; (c) V. S. P. K. Neti, X. F. Wu, S. G. Deng and L. Echegoyen, *Polym. Chem.*, 2013, **4**, 4566; (d) R. K. Totten, Y. S. Kim, M. H. Weston, O. K. Farha, J. T. Hupp and S. T. Nguyen, *J. Am. Chem. Soc.*, 2013, **135**, 11720; (e) S. Wan, F. Gándara, A. Asano, H. Furukawa, A. Saeki, S. K. Dey, L. Liao, M. W. Ambrogio, Y. Y. Botros, X. Duan, S. Seki, J. F. Stoddart and O. M. Yaghi, *Chem. Mater.*, 2011, **23**, 4094; (f) X. M. Liu, H. Li, Y. W. Zhang, B. Xu, A. Sigen, H. Xia and Y. Mu, *Polym. Chem.*, 2013, **4**, 2445.
- (a) F. J. Uribe-Romo, C. J. Doonan, H. Furukawa, K. Oisaki and O. M. Yaghi, *J. Am. Chem. Soc.*, 2011, **133**, 11478; (b) D. N. Bunck and W. R. Dichtel, *J. Am. Chem. Soc.*, 2013, **135**, 14952.
- A. Nagai, X. Chen, X. Feng, X. Ding, Z. Guo and D. Jiang, *Angew. Chem., Int. Ed.*, 2013, **52**, 3770.
- B. P. Biswal, S. Chandra, S. Kandambeth, B. Lukose, T. Heine and R. Banerjee, *J. Am. Chem. Soc.*, 2013, **135**, 5328.
- (a) G. M. Ucoski, F. S. Nunes, G. DeFreitas-Silva, Y. M. Idemori and S. Nakagaki, *Appl. Catal., A*, 2013, **459**, 121; (b) T. Poursaberi, M. Hassanisadi, K. Torkestani and M. Zare, *Chem. Eng. J.*, 2012, **189**, 117; (c) M. Moghadam, S. Tangestaninejad, V. Mirkhani, I. Mohammadpoor-Baltork and M. Moosavifar, *J. Mol. Catal. A: Chem.*, 2009, **302**, 68; (d) D. H. Shen, L. T. Ji, Z. G. Liu, W. B. Sheng and C. C. Guo, *J. Mol. Catal. A: Chem.*, 2013, **379**, 15.
- C. Zou, T. Zhang, M. H. Xie, L. Yan, G. Q. Kong, X. L. Yang, A. Ma and C. D. Wu, *Inorg. Chem.*, 2013, **52**, 3620.
- J. P. Collman, X. Zhang, V. J. Lee, E. S. Uffelman and J. I. Brauman, *Science*, 1993, **261**, 1404.
- J. Xie, Y. J. Wang and Y. Wei, *Catal. Commun.*, 2009, **11**, 110.